Sensors and Materials, Vol. 34, No. 5 (2022) 1869–1877
MYU Tokyo

S & M 2937

Contactless Electrostatic Vibration Energy Harvesting Using Electric Double Layer Electrets

Daisuke Yamane[1,2*] Kentaro Tamura,[1] Keigo Nota,[1] Ryuta Iwakawa,[2]
Cheng-Yao Lo,[3,4] Kazumoto Miwa,[5] and Shimpei Ono[5]

[1]Graduate School of Science and Engineering, Ritsumeikan University,
1-1-1 Noji-Higashi, Kusatsu, Shiga 525-8577 Japan
[2]Department of Mechanical Engineering, College of Science and Engineering, Ritsumeikan University,
1-1-1 Noji-Higashi, Kusatsu, Shiga 525-8577 Japan
[3]Institute of NanoEngineering and MicroSystems, National Tsing Hua University, Hsinchu 300044 Taiwan
[4]Department of Power Mechanical Engineering, National Tsing Hua University, Hsinchu 300044 Taiwan
[5]Materials Science Research Laboratory, Central Research Institute of Electric Power Industry,
Yokosuka, Kanagawa 240-0196 Japan

(Received April 22, 2022; accepted April 28, 2022)

Keywords: contactless, electric double layer electret, electrostatic, energy harvester, vibration energy harvesting

In this paper, we present demonstration results for a contactless electrostatic vibration energy harvester (E-VEH) using electric double layer electrets (EDLEs). We, for the first time, utilize the surface potential of EDLEs to generate electrostatic induction currents for contactless VEH devices. A proof-of-concept in-plane EDLE E-VEH is designed and developed using precision machining technology. An array of EDLEs is developed and the surface potential is measured under atmospheric conditions and found to be −1 V on average. The proposed contactless energy harvesting method using the electrostatic induction of EDLEs is successfully demonstrated by performing vibration experiments under atmospheric conditions. We confirm a typical output current of about 2 pA (peak-to-peak) with a load resistance of 1 MΩ at an input acceleration of 1 G with a frequency of 155 Hz. The proposed vibration energy harvesting mechanism is expected to expand the range of environments in which E-VEHs are used with EDLEs.

1. Introduction

The number of sensors placed in humans, objects, and the environment to convert real physical information associated with human society into digital data is expected to exceed 1 trillion in the future.(1) Many such sensors will be used with wireless IoT nodes connected to Internet networks. Wireless technology eliminates the need for the wiring of power cables and signal lines, reducing environmental impact and system costs and expanding the range of environments in which sensors can be placed. Currently, batteries are used to energize wireless sensor nodes, but if the number of such nodes becomes enormous, it will be difficult to manually replace or recharge batteries. In addition, if a large number of wireless IoT sensor nodes with

*Corresponding author: e-mail: dyamane@fc.ritsumei.ac.jp
https://doi.org/10.18494/SAM3945

ISSN 0914-4935

batteries are deployed, many of them will remain in the environment as uncollected waste, with the chemicals in the batteries having an adverse environmental impact.

Energy harvesting (EH) is a promising technology for solving these IoT power supply issues[2,3] by converting minute amounts of various forms of environmental energy that exist around us into electrical energy. Environmental energy includes light from the sun and indoor lighting, vibrations generated by infrastructure and machinery, biological motion, waste heat, and electromagnetic waves used by wireless communications. Among the wide variety of EH technologies, vibration energy harvesters (VEHs), [4–6] which use environmental vibrations that exist day and night, indoors and outdoors, and even in dark places,[7] are attracting attention as stand-alone power sources for wireless IoT sensor nodes that can operate in any environment. The frequency of environmental vibrations is mainly below 200 Hz and even that of mechanical vibrations is about 1 kHz or less.[6,8] VEHs convert kinetic vibration energy into electricity, and electrostatic VEHs (E-VEHs) using electrostatic induction are advantageous for generating power from environmental vibrations because of their high output power density at low frequencies compared with other methods.[6] E-VEHs utilize electrets, which are dielectrics that can semi-permanently retain their charges or dipoles. Conventionally, electrets require high-temperature charging processes[5,6] of typically 100 to several hundred degrees Celsius, at which low-melting-point materials or low-heat-resistance polymers cannot be used.

Recently, electric double layer electrets (EDLEs) have been developed for VEH applications.[9] EDLEs are made of ionic liquids and can be developed at room temperature. In the EDLE-based VEHs reported so far, the EDLEs and their counter electrodes are in physical contact when vibration is applied, and several factors affect the power generation. The frequency of environmental vibrations that can be used with these contact-type EDLE VEHs has been on the order of 10 Hz or less.[9–12]

In this work, we propose a contactless EDLE E-VEH and realize its operation with the aim of expanding the range of environments in which EDLE E-VEHs can be used. An overview of this study and the preparatory experiments were presented in our previous report.[13] Here, we describe the design methodology for the proof-of-concept device, report in detail the measurement results of device characteristics, and discuss methods for further increasing the output power.

2. Concept

Table 1 shows the operation modes of electret-based VEHs. VEHs using conventional electrets such as CYTOP and SiO_2 are contact types using electrostatic induction with the

Table 1
(Color online) Operation modes of electret-based VEHs.

		Electret-based VEH	
		Conventional Electrets (CYTOP, SiO_2, etc.)	**EDLE**
Operation Mode	**Contact**	✓	✓ (f_{op} < several tens of hertz)
	Contactless	✓ (f_{op} is unlimited)	**This Work** (EDLE E-VEH)

f_{op} : Operation Frequency

combination of piezoelectricity or triboelectricity[14,15] or contactless types employing electrostatic induction, where the moving electrodes and electrets do not come into contact when vibration is applied.[5,6] On the other hand, only the types in which the moving electrodes and electrets are in physical contact have been reported for VEHs using EDLEs.[9–12] Multiple factors such as piezoelectricity, triboelectricity, and electrostatic induction contribute to the contact-type power generation.[12] In the case of contact-type VEHs with EDLEs, moving electrodes operate in nonresonant modes, and the vibration frequencies are typically limited to 1 to several tens of Hz.[9–12] To expand the use environment in terms of the operating frequency, we propose a contactless EDLE E-VEH. It is also expected to be possible to use the resonant mode of the contactless EDLE E-VEH to improve the output power when the vibration frequency matches the resonance frequency of the harvester.[4–6]

3. Method

The power generation principle of the proposed contactless EDLE E-VEH is schematically shown in Fig. 1. Unlike contact-type VEHs, there is always an air gap between the movable electrode and the electret. The fixed charges on the surface of the EDLE generate induced charges on the moving electrode. When vibration is applied, the overlap area between the movable electrode and the EDLE varies, which changes the amount of induced charge, and electrical current flows to the external load. This power generation principle has been widely employed in E-VEHs using electrets other than EDLEs.[4–6] To use this methodology, it is necessary to develop EDLEs with controlled dimensions and to confirm their surface potential. However, the surface potential of EDLEs has not been reported so far.

As shown in Fig. 2, a 500-mm-thick Teflon spacer was used to develop EDLEs, as reported elsewhere.[10] The EDLEs consist of an ionic liquid [(2-methacryloyloxyethyl) trimethylammonium bis (trifluoromethanesulfonyl) imide] and acrylate polymer, both of which have unsaturated bonds in the molecular structures. In the preparation of an ionic gel, the first step is to dissolve acrylate polymers with acetonitrile, and then the ionic liquid and a polymerization initiator are added. The ionic gel is placed between an indium tin oxide (ITO) electrode and a gold electrode with a gap made by the Teflon spacer, where a bias voltage of 3 V is applied to the ionic gel. This bias voltage is applied until the current between the two electrodes starts to saturate so that both

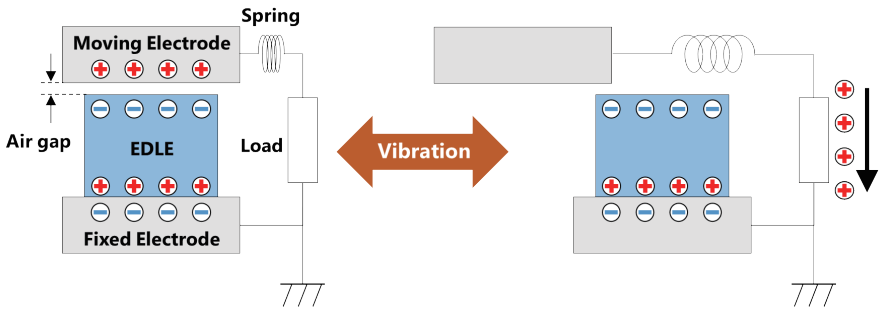

Fig. 1. (Color online) Power generation principle of the proposed contactless EDLE E-VEH.

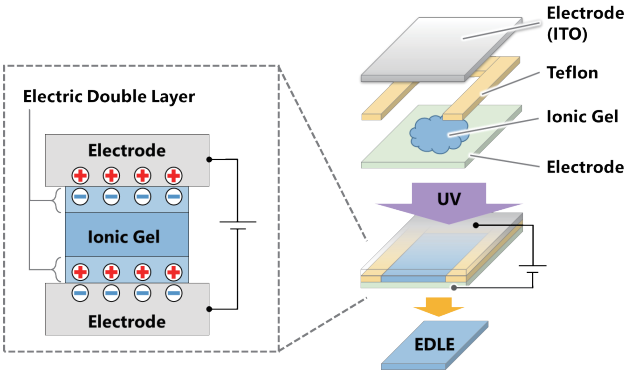

Fig. 2. (Color online) EDLE process flow.

cations and anions are redistributed to form EDLs at the interfaces between the ionic gel and the electrodes. Finally, we irradiate UV light (235 nm) to accelerate polymerization to develop an EDLE, as reported elsewhere.[16] Figure 3 shows the developed EDLEs with an area of 5 × 5 mm^2 and a thickness of 500 mm. As shown in Fig. 4, an electrostatic voltmeter (Trek 344, Advanced Energy) was used to evaluate the EDLE surface potential, and the average surface potential of the anion sides of the developed EDLEs was measured under atmospheric conditions to be −1 V.

Next, we proposed and designed a proof-of-concept EDLE E-VEH, schematic images of which are shown in Fig. 5. As shown in Fig. 5(a), the moving electrode is placed on the EDLE through an air gap, and the air gap can be adjusted by changing the thickness and number of the spacers. In this experiment, we used 800-mm-thick spacers. The screws and spacers are insulators, and thus the moving electrode and the EDLEs on the ITO electrode are electrically isolated. The movable electrode has through holes, each with the same area as a 5 × 5 mm^2 EDLE. When in-plane vibration is applied, the overlap area between the movable electrode and the out-of-plane electrode changes, generating an induced current. As shown in Fig. 5(b), four sets of through holes were made in the movable electrode to fit an electret sample with a 2 × 2 array of 5 × 5 mm^2 EDLEs spaced 5 mm apart. To utilize mechanical resonance, the design specification for the resonant frequency in the in-plane direction was set at 200 Hz or lower, taking into account the frequency bandwidth of environmental vibrations.[6,8] As illustrated in Fig. 5, eight cantilever beams of length l, width w, and thickness t are utilized to form springs. If the truss structure connecting four cantilever beams has a sufficiently larger second moment of area around the z-axis than the cantilever beams, then the composite spring constant k_x in the x-direction can be expressed as

$$k_x = \frac{2Ew^3t}{l^3}, \tag{1}$$

where E is Young's modulus.[17] Thus, the resonant frequency f_{res_x} of the moving electrode of mass m in the in-plane direction is

$$f_{res\_x} = \frac{1}{2\pi}\sqrt{\frac{k_x}{m}}. \tag{2}$$

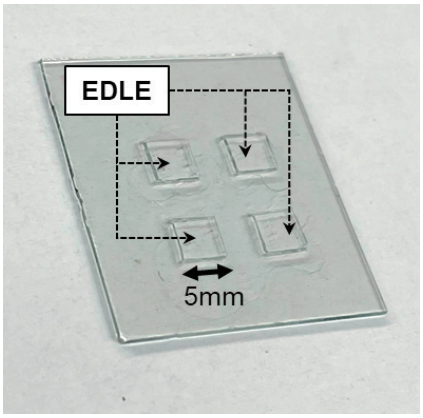

Fig. 3. (Color online) Developed EDLEs.

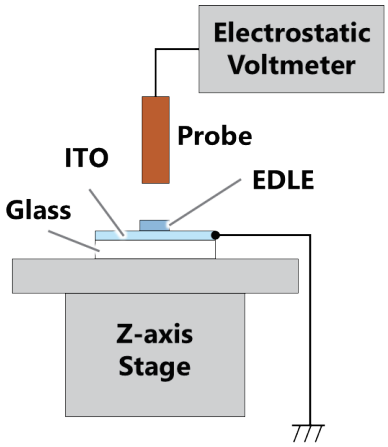

Fig. 4. (Color online) Experimental setup for surface potential measurement.

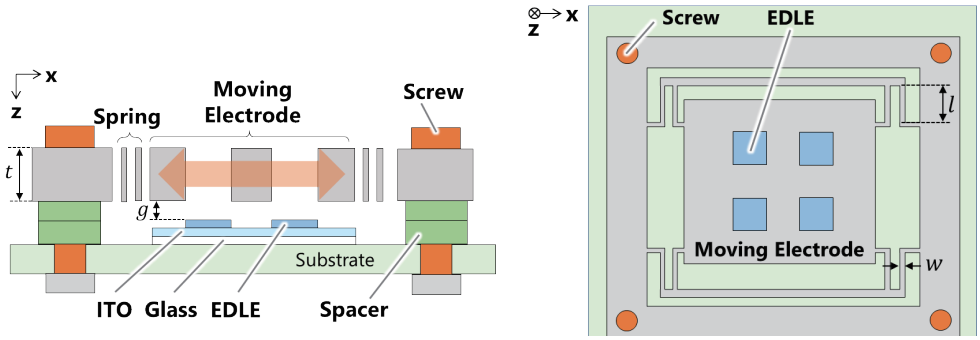

Fig. 5. (Color online) EDLE E-VEH schematics. (a) Cross section and (b) top view.

In addition to the above analysis, a finite element method simulation using COMSOL Multiphysics 5.6 was performed, as shown in Fig. 6. The density and Young's modulus of the phosphor bronze (C5191) used as the structural material were 8.83×10^3 kg/m^2 and 110 GPa, respectively. Table 2 shows the design results for the in-plane resonance frequencies (f_{res_x}) of the EDLE E-VEH used. In this design, l, w, and t were set to 13, 0.4, and 0.5 mm, respectively. The spring constant in the z-direction is 5.0×10^3 N/m, and the displacement due to gravity at 1 G (G = 9.8 m/s^2) is about 4.5 mm for the spacer thickness of 800 mm and EDLE thickness of 500 mm, which is negligible.

Photographs of the assembled EDLE E-VEH are shown in Fig. 7. The moving electrode was developed by electrical discharge machining. As shown in Fig. 7(a), the four sets of EDLEs were placed under the through-holes of the moving electrodes. The air gap between the movable electrode and the EDLE is approximately 300 mm because a 700-mm-thick glass substrate, 500-mm-thick EDLEs, and two 800-mm-thick spacers are used, as shown in Fig. 7(b).

Table 2
In-plane resonant frequency of EDLE E-VEH.

	Target specification	Analysis	FEM simulation
In-plane resonant frequency f_{res_x} (Hz)	<200	187	159

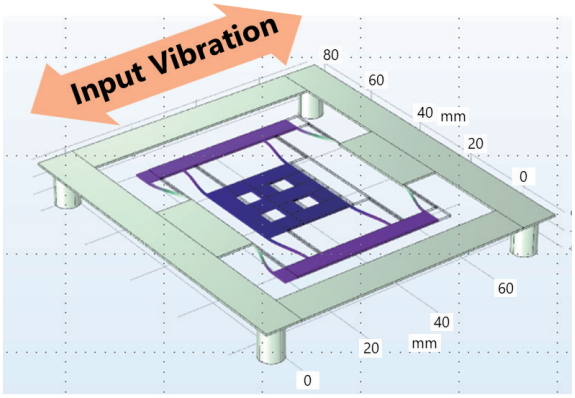

Fig. 6. (Color online) Simulation model of EDLE E-VEH.

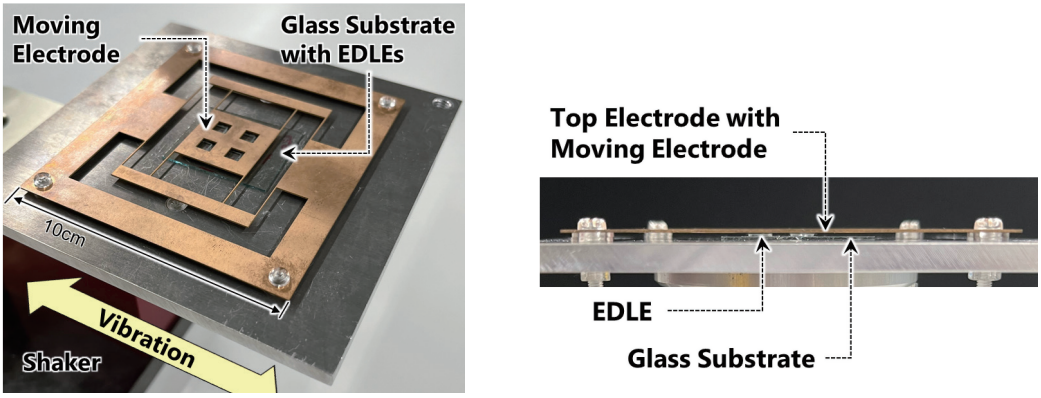

(a) (b)

Fig. 7. (Color online) Developed EDLE E-VEH. (a) Top view and (b) cross section.

4. Evaluation Results

Figure 8 shows the experimental setup for electrostatic induction current measurements. The developed EDLE E-VEH was fixed to a jig on a shaker (WaveMaker05, ASAHI SEISAKUSYO Ltd.) so that in-plane vibration could be applied. The ITO electrode at the bottom of each EDLE was electrically grounded during the measurement. In this experiment, the moving electrode was placed over the anion sides of the EDLEs through an air gap. The currents induced through the load resistance were measured with an I/V amplifier (CA5350, NF Corp.) and an oscilloscope (DLM2022, Yokogawa Test & Measurement Corp.) when vibration was applied. This experiment was carried out under atmospheric conditions due to the constraints of the experimental setup. Consequently, the electrical properties of the EDLEs degrade with time,[12] making it difficult to quantitatively evaluate the performance of the energy harvester. Thus, the aim of this study is

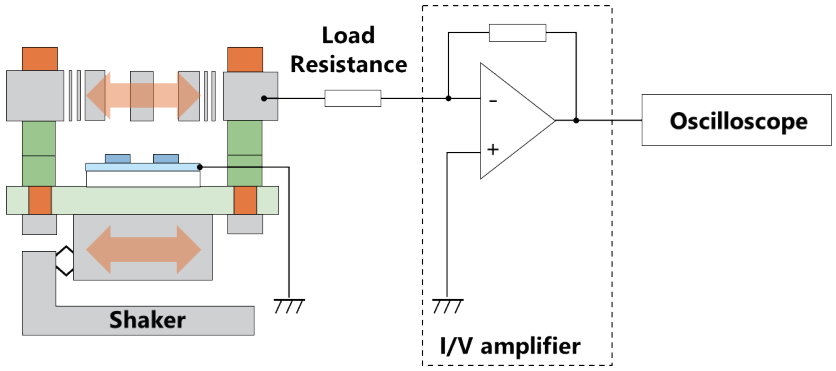

Fig. 8. (Color online) Experimental setup for electrostatic induction current measurement.

only to demonstrate the operation of the proposed power generation principle.

The measured output current waveform is shown in Fig. 9(a). A sinusoidal acceleration with a frequency of 155 Hz and an amplitude of 1 G was applied, and an induced current waveform with the same frequency as the input acceleration was observed. The amplitude of the measured induced current increased with the input acceleration amplitude as shown in Fig. 9(b). This is because as the input acceleration increases, the displacement of the movable electrode increases and the change in the overlap area between the EDLE and the movable electrode increases, thereby increasing the amount of induced charge. To determine whether the output current characteristic is close to saturation, it is also necessary to evaluate the output current at a lower acceleration range. However, at present, when acceleration below 0.2 G is applied, the current waveform is buried in noise and cannot be observed. In the future, it will be necessary to prepare an experiment condition in which the surface potential of EDLE does not deteriorate easily, such as in inert gas or under vacuum, to make more precise measurements. As can be seen from Fig. 9(c), the induced current increased as the frequency of the input acceleration approached 159 Hz, which is the in-plane resonant frequency of the movable electrode. This frequency response is due to the fact that the displacement of the movable electrode at resonance is multiplied by the quality factor compared with that at nonresonance.[6] Figure 9(d) shows the relationship between the measured output power density and the load resistance. In this case, the total volume of four $5 \times 5 \times 0.5$ mm^3 EDLEs was used to calculate the output power density, since part of the mechanical structure of the device also serves as the experimental apparatus. The output power density is linearly scaled (2×10^{-7} fW/cm^3/G^2/Ω) with the load resistance. Similarly to other VEHs,[10,11] the output power can be designed by tuning the load resistance.

5. Discussion

To further increase the output power, several techniques can be considered. The amount of induced charge increases as the capacitance or potential difference between the fixed electrode and the EDLE increases. One method to increase the capacitance is to use microfabrication technologies such as MEMS processes,[18] which allow VEH devices to be manufactured in micrometer or submicrometer dimensions. For example, if the air gap, currently made with

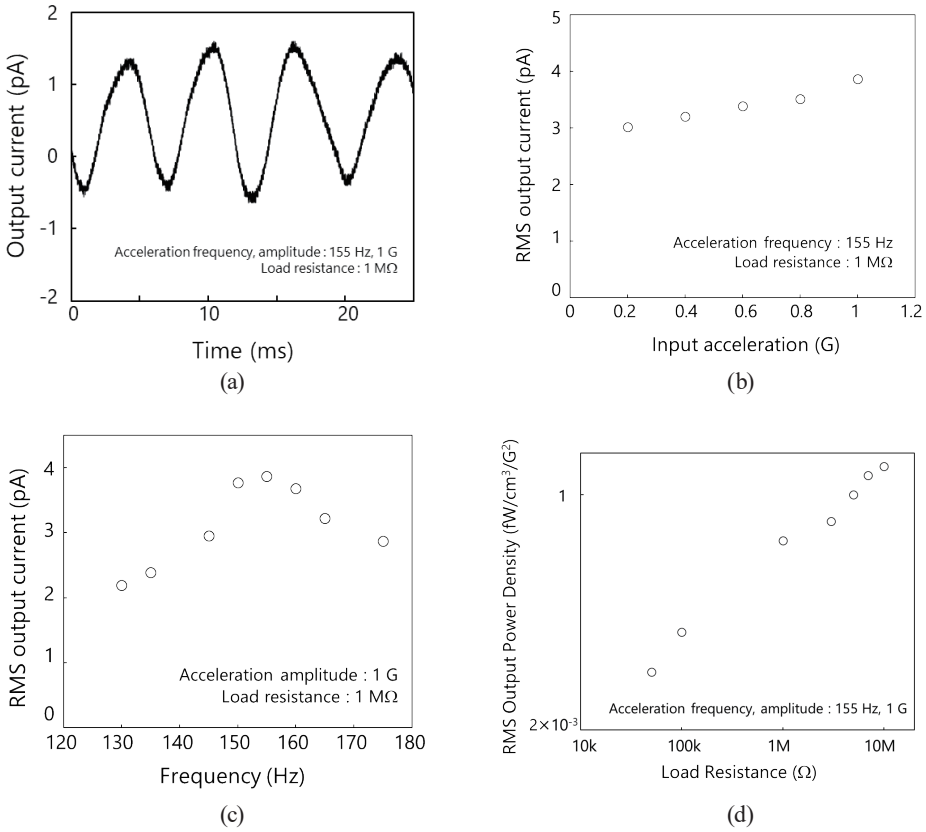

Fig. 9. Measurement results. (a) Output current waveforms, (b) output current as a function of input acceleration amplitude, (c) output current as a function of input acceleration frequency, and (d) output power density as a function of load resistance.

spacers and screws, is fabricated with dimension on the order of 1 or 10 mm, the capacitance can be increased by two or three orders of magnitude. Techniques for manufacturing EDLEs in micrometer dimensions have recently been developed,[12] and the integration of these microfabrication techniques is expected to further increase the output power. Appropriate packaging technology for the EDLE E-VEH devices is also essential. Currently, power generation experiments are being conducted under atmospheric conditions due to the limitations of the experimental systems, but the surface potential of EDLEs decreases rapidly over time in the atmosphere.[12] Therefore, it is necessary to evaluate the performance of devices sealed in an inert gas or vacuum to optimize the power generation performance, as well as carry out a theoretical study.

6. Conclusions

We proposed a contactless EDLE E-VEH to expand the range of environments in which EDLE E-VEHs can be used. A proof-of-concept device for EH using in-plane vibration was developed through precision machining technology. The average surface potential of the developed EDLEs was measured under atmospheric conditions to be −1 V. Contactless EH based on the electrostatic induction of EDLEs was successfully demonstrated by artificially applying

vibration. We confirmed a typical output current of about 2 pA (peak-to-peak) with a load resistance of 1 MΩ at an input acceleration of 1 G with the frequency of 155 Hz. The proposed contactless EH mechanism is expected to contribute to expanding the range of usage environments of E-VEHs with EDLEs.

Acknowledgments

This work was supported in part by JST CREST Grant Number JPMJCR21Q2, Japan and JSPS 22H01929, Japan.

References

1 S. Kaminaga: Sens. Mater. **30** (2018) 723. http://dx.doi.org/10.18494/SAM.2018.1814
2 H. Sun, M. Yin, W. Wei, J. Li, H. Wang, and X. Jin: Microsyst. Technol. **24** (2018) 2853. https://doi.org/10.1007/s00542-018-3763-z
3 H. Akinaga: Jpn. J. Appl. Phys. **59** (2020) 110201. https://doi.org/10.35848/1347-4065/abbfa0
4 S. P. Beeby, M. J. Tudor, and N. M. White: Meas. Sci. Technol. **17** (2006) R175. http://doi.org/10.1088/0957-0233/17/12/R01
5 Y. Suzuki: IEEJ Trans. Elec. Electron. Eng. **6** (2011) 101. https://doi.org/10.1002/tee.20631
6 H. Toshiyoshi, S. Ju, H. Honma, C.-H. Ji, and H. Fujita: Sci. Technol. Adv. Mater. **20** (2019) 124. https://doi.org/10.1080/14686996.2019.1569828
7 S. Roundy, P. K. Wright, and J. Rabaey: Meas. Sci. Technol. **26** (2003) 1131. https://doi.org/10.1016/S0140-3664(02)00248-7
8 P. D. Mitcheson, E. M. Yeatman, G. K. Rao, A. S. Holmes, and T. C. Green: Proc. IEEE **96** (2008) 1457. https://doi.org/10.1109/JPROC.2008.927494
9 S. Ono, K. Miwa, J. Iori, H. Mitsuya, K. Ishibashi, C. Sano, H. Toshiyoshi, and H. Fujita: J. Phys.: Conf. Ser. **773** (2016) 012074. https://doi.org/10.1088/1742-6596/773/1/012074
10 C. Sano, H. Mitsuya, S. Ono, K. Miwa, H. Toshiyoshi, and H. Fujita: Sci. Technol. Adv. Mater. **19** (2018) 317. https://doi.org/10.1080/14686996.2018.1448200
11 S. Yamada, H. Mitsuya, S. Ono, H. Toshiyoshi, and H. Fujita: IEEJ Trans. Sens. Micromach. **139** (2019) 7. https://doi.org/10.1541/ieejsmas.139.7
12 T. Iida, T. Tsukamoto, K. Miwa, S. Ono, and T. Suzuki: Sens. Mater. **31** (2019) 2527. https://doi.org/10.18494/SAM.2019.2309
13 K. Tamura, K. Nota, K. Miwa, S. Ono, and D. Yamane: Proc. 2021 IEEE 20th Int. Conf. Micro and Nanotechnology for Power Generation and Energy Conversion Applications (PowerMEMS) (Online, 2021) 100–103. https://doi.org/10.1109/PowerMEMS54003.2021.9658364
14 Y. Zhang, C. R. Bowen, S. K. Ghosh, D. Mandal, H. Khanbareh, M. Arafa, and C. Wan: Nano Energy **57** (2019) 118. https://doi.org/10.1016/j.nanoen.2018.12.040
15 Y. Wu, Y. Hu, Z. Huang, C. Lee, and F. Wang: Sens. Actuators, A **271** (2018) 364. https://doi.org/10.1016/j.sna.2017.12.067
16 S. Ono and K. Miwa: Sens. Mater. **34** (2022) 1853.
17 G. K. Fedder: Ph.D. Thesis (University of California, Berkeley, 1994).
18 D. Yamane, H. Kayaguchi, K. Kawashima, H. Ishii, and Y. Tanaka: Appl. Phys. Lett. **119** (2021) 254102. https://doi.org/10.1063/5.0072596